

# We are IntechOpen, the world's leading publisher of Open Access books Built by scientists, for scientists

6,900

Open access books available

186,000

International authors and editors

200M

Downloads

Our authors are among the

154

Countries delivered to

TOP 1%

most cited scientists

12.2%

Contributors from top 500 universities



WEB OF SCIENCE™

Selection of our books indexed in the Book Citation Index  
in Web of Science™ Core Collection (BKCI)

Interested in publishing with us?  
Contact [book.department@intechopen.com](mailto:book.department@intechopen.com)

Numbers displayed above are based on latest data collected.  
For more information visit [www.intechopen.com](http://www.intechopen.com)



# The Tension over the Hubble-Lemaitre Constant

*Michael L. Smith and Ahmet M. Öztaş*

## Abstract

Astronomers continue the search for better a Hubble-Lemaitre constant,  $H_0$ , value and other cosmological parameters describing our expanding Universe. One investigative school uses ‘standard candles’ to estimate distances correlated with galactic redshifts, which are then used to calculate  $H_0$  and other parameters. These distance values rely on measurements of Cepheid variable stars, supernovae types Ia and II or HII galaxies/giant extra-galactic HII regions (GEHR) or the tip of red giant star branch to establish a distance ‘ladder’. We describe some common pitfalls of employing log-transformed HII/GEHR and SNe Ia data rather than actual distances and suggest better analytical methods than those commonly used. We also show that results using HII and GEHR data are more meaningful when low quality data are discarded. We then test six important cosmological models using HII/GEHR data but produce no clear winner. Groups utilising gravitational waves and others measuring signals from the cosmic microwave background are now at odds, ‘tension’, with those using the SNe Ia and HII data over Hubble-Lemaitre constant values. We suggest a straightforward remedy for this tension.

**Keywords:** Hubble constant, Hubble-Lemaitre constant, cosmological parameters, distance ladder, distance scale, data analysis, supernova, HII galaxies, luminosity distance, redshift

## 1. Introduction

Some important goals of cosmology are determination of values for the local Hubble-Lemaitre constant,  $H_0$ , the average Universe matter density,  $\rho$ , as well as confirmation, or not, of the cosmological constant,  $\Lambda$ . Important tools are information emanating from supernovae types Ia (SNe Ia) and II (SNe II) explosions,  $\gamma$ -ray bursts and redshifts,  $z$ , combined with distance determinations to closer Cepheid variable stars [1, 2]. Estimates are also made using data from single events; the cosmic microwave background (CMB) [3, 4] and gravitational waves combined with electromagnetic detection [5, 6]. Values for  $H_0$  as determined by different research groups do not closely match and the situation is described as ‘tension’; the differences being ascribed to the lack of dark energy and the larger matter density in our early Universe [7] or perhaps to a ‘local hole’ and discrepancies between parallax distance estimates [8]. The different values for  $H_0$  are puzzling for one might expect larger values towards recombination than today but the reverse is reported and the difference between  $H_0$  values is increasing with more reports [9]. The controversy has generated considerable interest for astrophysics including Internet blogs and one video with over 135,000 views [10].

Results from the CMB investigations depend on exacting measurements of tiny, low-energy fluctuations modelled with at least 6 parameters, demanding many ‘priors’ (fixed-valued parameters) and cannot realistically discriminate between models since there are many parameter combinations able to fit many models [3, 11]. Results from SNe Ia investigations are model-dependent, rely on 2 or 3 parameters as published, but in reality 4 or 5 parameters are used for modelling and the belief that most SNe Ia events are uniform and similar. Systematic errors of collection and analysis are still being discovered, corrected or culled from data [12].

Estimates of SNe Ia distances typically rely on nearby Cepheid variable star distances which are still being adjusted [13, 14]. In addition, the methods used for evaluations of the SNe Ia data and claims therefrom have been repeatedly questioned [15, 16]. An independent method for estimating  $H_0$  has recently been published based on the characteristics of selected red giant stars [17, 18]. The value found,  $69.8 \text{ km s}^{-1} \text{ Mpc}^{-1}$  is close to the gravitational wave observation from a bi-neutron star collision,  $70 \text{ km s}^{-1} \text{ Mpc}^{-1}$ , much lower than calculated with SNe Ia data [1].

A pioneering effort is being made using the  $L(\text{H}\beta)\sigma$  distance estimator for giant extra-galactic HII regions (GEHR) and HII galaxies back to  $z \approx 2.3$  by a small group [19–23]; significantly further than SNe Ia observations. Several assumptions and adjustments to the data are necessary to allow use as astronomical distances analogous to SNe Ia data as done by Wei et al. [24]. The latter group presented results using the HII distance magnitudes,  $mag$ , and redshifts collected by the former group to investigate the properties of three important cosmological models. Their results suggest the  $Rh = ct$  model is a slightly better fit to the HII and GEHR data than two, well-known versions of the current standard ( $\Lambda$ CDM,  $\omega\Lambda$ CDM) models [25, 26]. The  $Rh = ct$  model is a special, geometrically flat version of an earlier proposal by John and Joseph [27]. This eternal, coasting, non-empty model has been recently reviewed [28]. Analyses using HII and GEHR data with the  $Rh = ct$  model suggest a  $H_0$  of  $62.3 \text{ km s}^{-1} \text{ Mpc}^{-1}$  [24, 29], which is lower than other recent reports but exactly the last estimate of Sandage and coworkers based on data from the Hubble telescope [30]. This low value is very important if true, because it greatly increases the Universe age allowing more time for initial star and galaxy formations. A second, recent study claims a selection of the HII data supports a flat Universe geometry and the  $Rh = ct$  model [31].

A major problem with these analyses is the use of a relationship commonly termed as a *Hubble diagram* or a *Hubble relationship* but is not. This relationship and analytic technique are commonly used in astrophysics and often leads to erroneous results. The real Hubble relationship is based on correlation between distance and galaxy recession velocity in accordance with fundamental physics [32]. Unfortunately, it is now common to correlate some version of  $\log(\text{distance})$ , usually termed *distance magnitude* or simply  $mag$ , with redshift ( $mag$  versus  $z$ , sometimes displayed as  $\log[z]$ ), and still use the term Hubble diagram to describe this correlation, which certainly is not distance versus velocity. Here we use the term *pseudo-H-routine* to describe the use of *distance mag* versus  $z$  and *H-routine* for luminosity distance,  $D_L$  versus relative recession velocity,  $v/v_0$  or  $a$ , the expansion factor.

There are many drawbacks using the pseudo-H-routine for model testing. First, distance is a physical metric but  $mag$  is not. Second, this routine non-uniformly compresses data dispersion and standard errors; errors of distant observations are systematically compressed over errors of more nearby emissions and will exacerbate skewness [33]. Using weighed regression analysis the pseudo-H-routine incorrectly emphasises the more imprecise, distant data, SNe or HII, which often leads to incorrect regression minima and results [34, 35]. Third, the best data pair, recession velocity and position of earth or the local group (1,0) without error, cannot be used

with the pseudo-H-routine, the distance becoming  $-\infty$ ; this exclusion can never be justified. Fourth, because the errors have been compressed, goodness of fit estimates are not properly distributed, are both smaller with more similar values, complicating model discrimination. Fifth, information from both intercepts are lost and cannot be recovered. If the pseudo-H-routine were valid, parameter estimates should be similar between the Hubble relationship and the pseudo-H-routine, but are not. Here and for other examples using SNe Ia data, the two analytic methods do not agree [16, 36].

There are many reasons to perform regression analysis using luminosity distance versus expansion factor ( $D_L$  versus  $a$ , H-routine) rather than  $mag$  versus  $z$ . First, the real distances and errors are used rather than perturbations. This allows examination of the real data dispersion and proper estimation of regression best fit. Second, more realistic measurement errors of distant objects are used for H-routine and are not dampened. The best error estimates are required to properly employ weighed fitting for regression routines. Third, the very best data pair (1,0) without error, is automatically used and anchors the regression estimates. For cosmology the position and velocity of the earth, sun or local group, are the very best anchor and estimates of the origin can be estimated directly using the H-routine. Fourth, the H-routine comes with two intercepts, the position of the earth and the Universe age. With good data the latter may be guesstimated, being asymptotic, and the former may be used to judge the value of nearby distances. Fifth, the H-routine allows visual examination of the relative data worth, which is important when these are billions of years old. Some SNe Ia and HII emissions display standard deviations similar to the Universe age. Sixth, the difference between goodness of fit estimates, such as  $\chi^2$ , are not depressed, which eases objective model discrimination. We claim the famous presentation of Hubble is still valid and suggest analyses using the pseudo-H-routine should be avoided.

Here we first use the same routine as Wei et al. ( $mag$  versus  $z$ ) to check our methods. Next, to comply with the requirements of the H-routine, we calculate the luminosity distances,  $D_L$ , and use the related expansion factors to test six cosmological models. We begin using all 156 HII and GEHR observations [20, 22, 24] but find it necessary to parse the data to obtain worthwhile results so we are forced to discard about half the events even though we conservatively allow all data within 99.99% confidence or a Studentised limit of 1.5. After this we find our analyses can more easily discriminate the relative model worth. Our results only support the precedence of the  $Rh = ct$  model when all HII/GEHR data are used. When questionable data are discarded, the  $\omega\Lambda$ CDM model is a better fit to the HII/GEHR data, however, this model requires 4 free parameters and in reality 6 parameters which means it is a plastic model which overfits the data. We suggest more and better HII and GEHR data are needed before this independent tool can be confidently used for model discrimination.

## 2. Data, models and methods

### 2.1 HII and GEHR data

We use data;  $mag$ , standard deviations about  $mag$  and redshifts,  $z$ , adjusted to the local group rather than heliocentric, as tabulated by Wei et al. [24] with HII data from [20, 23] and data collected and analysed by [22]. The HII data are usually those with  $a < 0.85$  and the GEHR data are usually associated with  $a > 0.85$ . Not all values from [20] were used by Wei leaving a total of 156 HII/GEHR data pairs. For examination using the relationship of distance modulus,  $mag$  versus  $z$  the



pseudo-H-routine, we follow [24] with  $H_0$ , nuisance parameter and  $mag$  value adjustments during iterative regression calculations. For model examination using the H-routine, we calculate the actual distances,  $D_L$  in Mpc, with the usual relationship, Eq. (6) of [24] as

$$D_L = 10((mag - 25)/5) \quad (1)$$

where  $mag$  is the distance modulus. We perform  $H_0$  and  $D_L$  value and standard deviation re-adjustments during repetitive calculations followed by re-evaluation and recalculation of  $H_0$ ,  $D_L$  and associated estimated errors, since the values of  $mag$  and  $D_L$  are dependent on  $H_0$ ; details in [24]. The expansion factors  $a$ , strictly proportional to the recession velocities, are calculated from  $a = 1/(1 + z) = v/v_0$  and are not modified, since observational errors of redshift determinations are tiny compared to errors about  $D_L$ . Though this has been recently contested if the reader carefully examines the data they will agree with our assessment of relative error [37].

For regression using  $D_L$  versus  $a$  we check the consistency of the different data sets compiled in [24] by calculating the  $D_L$  versus  $a$  from the tabulated  $mag$  values, as per Eq. (1) and use the position and recession velocity of the local group (1,0) as the anchor. We also use the distance and expansion factor values for 10 nearby galaxies but found these unnecessary as anchors, details in the Results. We check several different data subsets and find the different subsets to be internally consistent, that is, displaying random distribution about the best fits with the exception of 25 observations from  $a < 0.86$  ( $z \approx 0.17$ ) of [23]. When only these values are tested with the local group as the ‘anchor’ the distances to generally unbelievably large with very large standard deviations and inconsistent with the anchor. Rather than systematically reducing the  $D_L$  values of distant emissions we use the 156 tabulated values from [24].

To suppress the influence of outliers we parse the data in two manners. For both situations we only discard data simultaneously failing three models,  $\Lambda$ CDM,  $\omega\Lambda$ CDM and  $Rh = ct$ , at all three  $H_0$  values of 74.3, 71.0, 62.3  $\text{km s}^{-1} \text{Mpc}^{-1}$ . For the first parse we discard those beyond the 99.99% limits ( $\approx 4\sigma$ ), leaving from 86 to 89 data pairs. For the second subset we discard data exhibiting  $ri/\sigma_i > 1.5$  (residual/standard deviation; the Studentised limit) [38], leaving 74 to 77 pairs. Even using our conservative parsing routines both methods trim a number of observations from  $0.85 < a < 1$ . After parsing we perform regression analyses using the H-routine.

## 2.2 Models

The models tested are based on the Friedmann-Lemaitre-Robertson-Walker (FLRW) universe; explanations can be found in sources [39–41]. This is by far the most useful model of cosmology and an early version was used by Einstein and de Sitter to model the Universe, subsection 2.2.4. We make the usual assumption for FLRW model parameter normalisation

$$1 = \Omega_m + \Omega_\Lambda + \Omega_k \quad (2)$$

where  $\Omega_m$ ,  $\Omega_\Lambda$ ,  $\Omega_k$  are normalised matter density, cosmological constant (dark energy) and spacetime curvature, respectively. Four models examined here presume flat spacetime geometry with  $\Omega_k = 0$ , Eqs. (3), (5), (7), and (10). We will not re-examine the HII/GEHR data using Eqs. (4), (6) and (8) which have been used by others many times.

### 2.2.1 Eternal coasting, $Rh = ct$ model

This is the preferred model of Melia and coworkers [28, 42] with only one free parameter,  $H_0$ , presuming a geometrically flat universe and we use the relationship

$$D_L = \frac{c}{H_0 a} \ln \frac{1}{a} \quad (3)$$

with  $a$  the expansion factor,  $c$  is lightspeed and the natural  $\ln$ . Eq. (2) may hold true testing this  $Rh = ct$  model with HII/GEHR and SNe Ia data but  $\Omega_m$ ,  $\Omega_k$  and  $\Omega_\Lambda$  are not explicit with this model so cannot be evaluated, leaving  $H_0$  as the single parameter. To use the  $mag$  with redshift,  $z$ , one must employ not Eq. (3) but with

$$mag = 5 \log \left( \frac{c(1+z)}{H_0} \right) \ln(1+z) + 25 \quad (4)$$

Using Eq. (4) allows presentation of the pseudo-H-diagram with HII/GEHR data as in [24] where it is labelled 'Hubble diagram' though not really a Hubble-type diagram [32].

### 2.2.2 The current standard model of cosmology, $\Lambda$ CDM

Called the standard model of cosmology by some, with two free parameters, after adjusting the data for the local value of  $H_0$  as

$$D_L = \frac{c}{H_0 a} \int_1^a \left( \frac{da}{a \sqrt{\frac{\Omega_m}{a} + (1 - \Omega_m)a^2}} \right) \quad (5)$$

where  $(1 - \Omega_m)$  represents the normalised  $\Omega_\Lambda$ . The effect of spacetime curvature,  $\Omega_k$ , is presumed negligible for a geometrically flat universe. What is used in practice are values for the *distance magnitude* with the  $mag$  and  $z$  data modelled with this equation

$$mag = 5 \log \left[ \frac{c(1+z)}{H_0} \int_0^z \left( \frac{dz}{\sqrt{(1+z)^2(1 + \Omega_m z) + 2(2+z)(1 - \Omega_m)}} \right) \right] + 25 \quad (6)$$

but this version is rarely made explicit. Typical diagrams using this relationship can be found in [1, 43] and in award winning articles [44], but these are not really Hubble-type diagrams.

### 2.2.3 The standard model allowing the equation of state (EoS), $\omega\Lambda$ CDM

This is a variant of the standard model with a parameter,  $\omega$ , directly effecting  $\Omega_\Lambda$  as in

$$D_L = \frac{c}{H_0 a} \int_1^a \left( \frac{da}{a \sqrt{\frac{\Omega_m}{a} + a^2(1 - \Omega_m)^{3(1+\omega)}}} \right) \quad (7)$$

where  $\omega$  is a parameter estimating the relative influences of dark energy  $p$  and  $\rho$  as  $(p = \omega\rho)_{de}$  being the dark energy equation of state. A flat universe geometry is preferred with  $\omega \approx -1$  being a target by many [40]. What is used in practice with the  $mag$  and  $z$  data is

$$mag = 5 \log \left[ \frac{c(1+z)}{H_0} \int_0^z \left( \frac{dz}{\sqrt{(1+z)^2(1+\Omega_m z) + 2(2+z)(1-\Omega_m)^{3(1+\omega)}}} \right) \right] + 25 \quad (8)$$

but this version, too, is almost never presented. The reader can see that it is possible to add an extra parameter as a simple term to Eqs. (3), (5) and (7) which may be evaluated as the intercept. Results presenting large intercept values means some form of systematic error is present in the data. It is meaningless to add an extra term to Eqs. (4), (6) and (8) since evaluation cannot be made at the origin, which is  $-\infty$  so one loses a simple method for evaluating data worth.

#### 2.2.4 The Einstein-de Sitter model, EdS

After consulting with E. Hubble and becoming a convert to the idea of a dynamic universe, Einstein reconsidered the basis for his field equation. He then dropped the cosmological constant,  $\Lambda$ , and solved his theory for an expanding universe consisting of only matter as reviewed in [45]. Einstein and de Sitter began with the assumptions of Friedmann demanding spacetime curvature due to the presence of matter, which we cast using the FLRW model as

$$D_L = \frac{c}{aH_0} \sinh \left[ \int_a^1 \left( \frac{da}{a \sqrt{\frac{\Omega_m}{a}}} \right) \right] \quad (9)$$

where we use the  $\sinh$  function for positive curvature. If we allow  $\Omega_m = 1$  the result is a relationship which we term the EdS model. We have previously pointed out this model functions very well describing the Universe using only nearby emissions,  $z < 0.10$  [46].

$$D_L = \frac{c}{aH_0} \sinh \left( \sqrt{1-a} \right) \quad (10)$$

#### 2.2.5 The cosmological general relativity model, CGR

The cosmological general relativity model is a recent introduction to this subject [47]. The Hubble velocity is used as a tool by CGR to aid solutions using a 5-dimensional tensor with some success. For instance, the CGR model has been successfully applied to the Tully-Fisher relationship describing spiral galaxies [48]. This model does not admit the existence of dark matter and since dark matter has not been confirmed by several sensitive, direct observational tests [49, 50] this constraint holds true, so this model deserves our consideration.

For estimating  $H_0$  using standard candles, the CGR model for a flat universe present

$$D_L = \left( \frac{c}{aH_0 \sqrt{1-\beta^2}} \right) \times \left( \frac{\sinh(\beta \sqrt{1-\Omega_\beta})}{\sqrt{1-\Omega_\beta}} \right) \quad (11)$$

where  $\beta$  is shorthand for

$$\beta = \frac{\left(\frac{1}{a}\right)^2 - 1}{\left(\frac{1}{a}\right)^2 + 1} \quad (12)$$

and  $\Omega_b$  is the estimate of baryonic (normal) matter, whereas  $\Omega_m$  applies to all matter types. The reader should remember that baryonic matter is supposedly only 15–20% as plentiful as dark matter.

### 2.2.6 The FLRW model, ST, with the term, $\Omega_k$ , for spacetime

This model, which we term ST, admits the influences of both matter and geometric curvature on universe expansion so the condition for normalisation is

$$1 = \Omega_m + \Omega_k. \quad (13)$$

This is a significant change from other models considered here since the ST model is not restricted to a flat universe but allows the spacetime curvature parameter,  $\Omega_k$ . For use with the HII and GEHR data we present the form which can be integrated numerically as

$$D_L = \frac{c}{H_0 a} \int_1^a \left( \frac{da}{a \sqrt{\frac{\Omega_m}{a} + (1 - \Omega_m)}} \right) \quad (14)$$

or can be integrated analytically [46]. Comparison of the above with Eq. (5) shows these be similar except replacement of the  $1 - \Omega_m$  term with  $(1 - \Omega_m)a^2$  if one presumes a flat universe and late dark energy. This model deserves consideration since a recent attempt to detect dark energy in a lab failed [51].

## 2.3 Methods

We first apply the pseudo-H-routine to the log-transformed data as per Eqs. (4), (6) and (8) to check our regression routines. The reader should note that not only are the dependent values transformed into a logarithmic metric but the abscissa is transformed from relative velocity into galactic redshift as another non-linear metric,  $z = v/v_0 - 1$ . We use a weighted, robust regression routine normalised as

$$1 = \sum_1^i \ln \left( 1 + \left( |y_i - \hat{y}_i|^2 \right) \right) \quad (15)$$

to minimise the Bayesian Information Criteria (BIC), the reduced  $\chi^2$  and outlier influence as per [38]. We report the values for  $\Delta\text{BIC}$  [52], and the reduced  $\chi^2$  as  $\chi^2/\text{DOF}$  where  $N$  is the number of data pairs,  $FP$  is the number of free parameters and  $\text{DOF}$  is the degree of freedom,  $\text{DOF} = N - FP$ . We then apply nonlinear regression using the H-routine and distance values,  $D_L$  with Eqs. (3), (5), (7), (9), (10) and (13) as per [32] both with and without intercepts.

Using all 156 data pairs and (1,0) for the position of the local group, most regressions using the H-routine present results with  $H_0 > 85 \text{ km s}^{-1} \text{ Mpc}^{-1}$  which we think unrealistic. The models present many shallow, local minima which is partly the result of the minuscule weights allowed the distant emissions with large associated errors. This makes model comparison difficult because unique, deep regression minima often cannot be found. We observe many values for  $D_L$  beyond the 99.99%



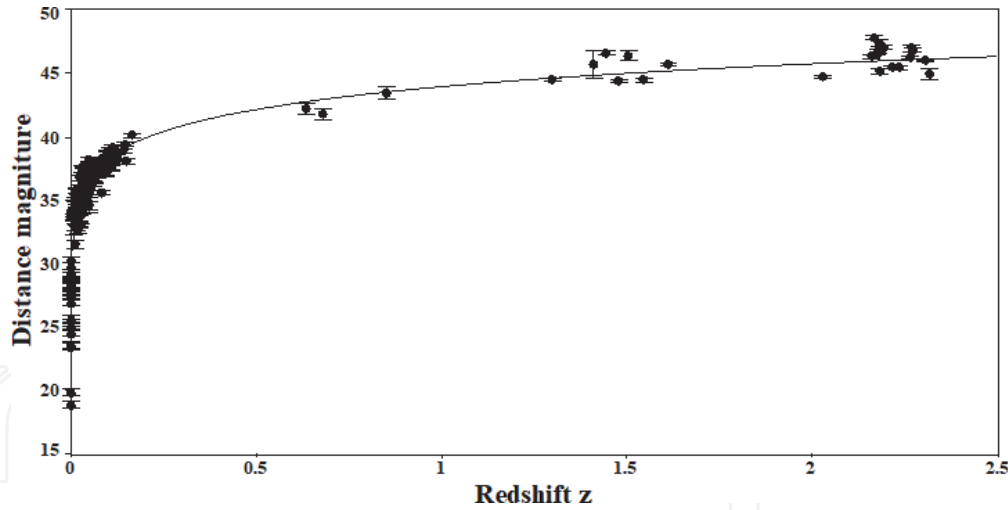


**Figure 1.**

Diagram of a pseudo-H-routine regression using all 156 HII and GEHR data. The line is the best fit of the  $\Lambda$ CDM model with  $H_0$  the prior at  $70.9 \text{ km s}^{-1} \text{ Mpc}^{-1}$ .

confidence interval with all models, and present data and results from regression with the  $\Lambda$ CDM model at  $H_0 = 70.9$  in **Figure 1** as one example. There are 68 values of  $D_L$  which lie outside the 99.99% confidence limits ( $\approx 4\sigma$ ). The standard deviations for many emission at  $z < 0.86$  are a large fraction of the Universe diameter and many  $D_L$  values lie well above the 99.99% confidence limit when there should only be one or two. For these reasons we decided to parse the data using two different conservative methods.

### 3. Results

We can reproduce the results of [24] using the routine of correlating  $mag$  versus  $z$  with adjustments of nuisance parameters. The data handling routines are checked by first using all 156 HII/GEHR observations and the pseudo-H-regression routine against reported results with Eqs. (4), (6) and (8). We find parameters and goodness of fit values very similar to those of [24]. We present diagrams of our regression using the  $\Lambda$ CDM model using all 156  $mag$  and redshift data pairs in **Figures 1** and **2**. We chose to display results from the standard model even though this is not the best fit with these data but because this model is the most popular. Note the standard deviations of distant emissions appear similar to those of more nearby events which is unrealistic. It is common knowledge that distant objects are more difficult to measure accurately than those nearby and measuring luminosity through billions of years of intergalactic dust must introduce more noise than for nearby emissions.

This problem is highlighted in **Figure 2** where it is obvious the standard deviations are very similar for nearby emissions and those at  $z > 1$ , which have travelled more than 6 billion light years. Also note the ordinate intercept cannot be displayed as (0,0), which is the location and relative velocity of the local group. This most accurate data pair cannot be used with this diagram type. Diagrams such as **Figures 1** and **2** using SNe Ia data have been used for presentation by many continuing to this day [1, 9, 43, 44, 53].

When we attempt regression following the robust H-routine with Eqs. (3), (5), (7), (9), (10) and (13) using all 156 data pairs plus the local group position (1,0), we fail to find satisfactory solutions at  $H_0 < 85 \text{ km s}^{-1} \text{ Mpc}^{-1}$ ; the high side of a realistic value. We attempt regression using many different data handling routines;

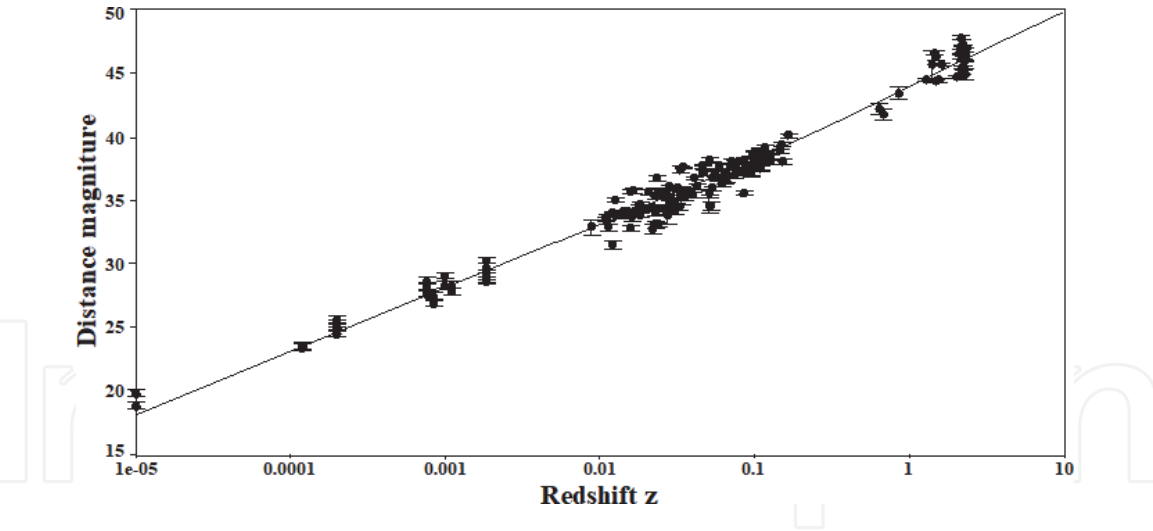


**Figure 2.**  
 Diagram of a pseudo-H-routine regression using all 156 HII and GEHR data. The centre line is the best fit of the  $\Lambda$ CDM model with  $H_0$  fixed at  $70.9 \text{ km s}^{-1} \text{ Mpc}^{-1}$ . Note the abscissa is  $\log_{10}$  format to better present nearby emissions.

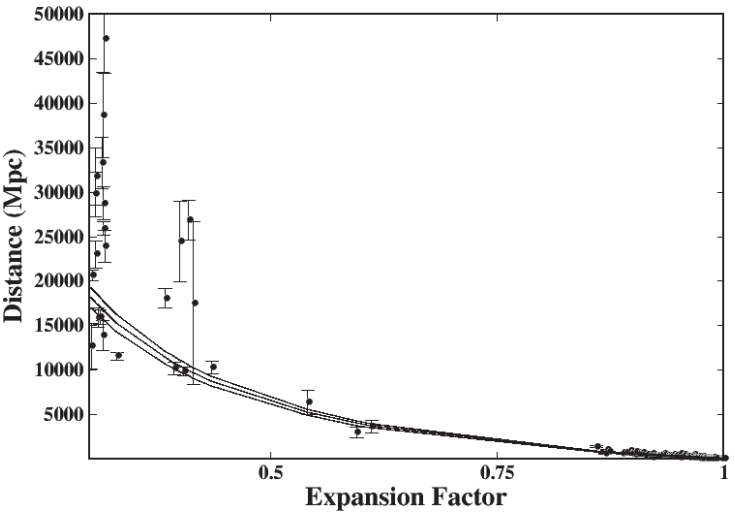


**Figure 3.**  
 The H-routine regression with all 157 HII and GEHR data plus 10 nearby galaxies. The centre line is the best fit for the  $R_h = ct$  model with  $H_0$  of  $65.9 \text{ km s}^{-1} \text{ Mpc}^{-1}$ . The outer lines are the  $\pm 99.99\%$  confidence intervals. The high side of the SD of the emission at  $a$  of 0.316 is not presented.

anchoring the HII/GEHR data in several manners, testing the data as various large segments, data without those of  $z > 0.18$  ( $a < 0.85$ ) with fixed or floating GEHR values or with and without the GEHR data. We tried including the positions of 10 nearby galaxies to improve the results with but to no avail.

We present one example of our many attempts in **Figure 3**, where we include data from those 10 neighbouring galaxies with fixed distances [54]. This presents relatively small scatter about the best fit for data  $a > 0.85$  but most values less than that are well above the best fit, that is, further distant than predicted and exhibiting large standard errors.

Examinations of both **Figures 3** and **4** reveal that nearby HII/GEHR sources display relatively small distance dispersion and errors, while ancient emissions are very scattered with very large estimated errors, as expected for difficult, distant observations. This presentation is very different from that displayed in **Figures 1** and **2**; the match of  $H_0$  at 71 was made by ‘massaging’ the *mag* data, that is by adjusting other parameters in order to recalculate the distances and associated standard deviations as necessary. The scattering data at  $a < 0.85$  [22], are the

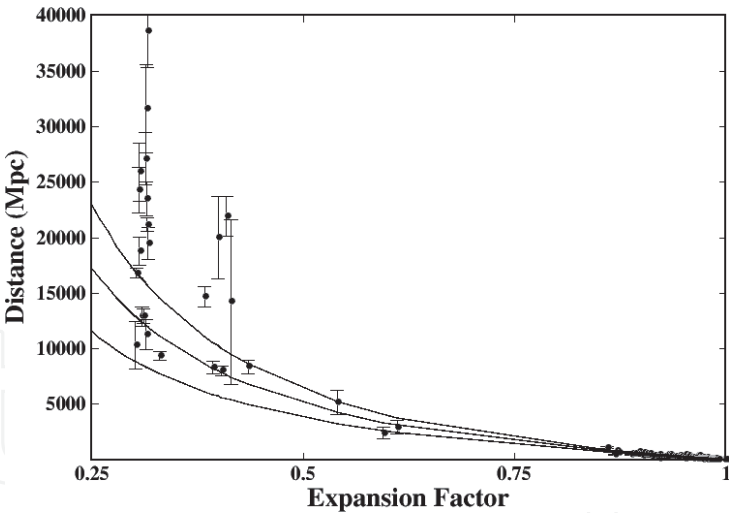


**Figure 4.** Diagram of an H-routine regression using all 156 HII and GEHR data plus the local group (1,0). The centre line is the best fit of the  $\Lambda$ CDM model with  $H_0$  fixed at  $70.9 \text{ km s}^{-1} \text{ Mpc}^{-1}$ . The outer lines border the  $\pm 99.99\%$  confidence interval. The high side of the standard deviation of the emission at  $a = 0.316$  at  $50,340 \text{ Mpc}$  is not presented. The Big Bang is at expansion factor 0, the local group of galaxies including our Milky Way is at 1,0.

primary reasons for our inability to reach believable best fits for these models when we attempt regression without strong restrictions or ‘priors’.

$H_0$  is the most important parameter for regression of FLRW-type models and is highly dependent on overall curvature of the regression, the slope if you will allow, and hence distant data quality. Because distant data are very noisy and suffer systematic error, these values are nearly ignored using weighed, computerised regression. The regression then ignores distant signals and becomes highly dependent on nearby SNe values. Unfortunately, this means the HII/GEHR data are currently of limited value for determining  $H_0$  and other cosmological parameters. Investigators relying on the pseudo-H-routine as displayed by **Figures 1** and **2** may claim [22], we are now in the era of ‘precision cosmology’ but evidence in these figures says otherwise.

For model comparisons in **Table 1** we list results from robust H-routine regressions with  $H_0$  of 71 as preferred by some working with HII/GEHR data [23]. Results are organised using the relative values of the calculated Bayesian information criteria ( $\Delta\text{BIC}$ ) [24] also with the reduced  $\chi^2$  values. The spread of both descriptors is much wider than calculated using the pseudo-H-routine [24], making

Model	$\Delta\text{BIC}$	$\chi^2/(\text{N-FP})$	$H_0^a$	$\Omega_m$	Intercept (Mpc)
$Rh = ct$	0	23.95	$71.0 \pm 2.1$	—	0.03
$\omega\Lambda\text{CDM}$	88.3	24.03	$71.0 \pm 8.3$	$1 \pm >1000$	0.03
CGR	91	21.9	$70.7 \pm 3.4$	$1 \pm 0.75$	0.07
$\Lambda\text{CDM}$	110	23.0	$70.9 \pm 2.9$	$1 \pm 0.28$	0
EdS	123	25.4	$71.3 \pm 2.4$	1	0.03
ST	140	22.6	$71.1 \pm 10.8$	$1 \pm 0.18$	0

<sup>a</sup> $\text{km s}^{-1} \text{ Mpc}^{-1}$ .  
 $\Delta\text{BIC}$  are the relative values of the Bayesian information criteria and  $\chi^2/(\text{N-FP})$  is the reduced sum of  $\chi^2$  with FP the number of free parameters.

**Table 1.** Analysis of  $D_L$  versus expansion factor with 157 observations including the local group (1.0) for regression minima close to  $71 \text{ km s}^{-1} \text{ Mpc}^{-1}$ .

discrimination between models easier. Note all intercepts are negligible indicating little systematic error in nearby signals.

The results for the standard model are eclipsed by those of the  $R_h = ct$  model when all 156 HII/GEHR values are used with the H-routine, **Table 1**. These strongly support the findings of [24], that is, if judged by the lowest value of  $\Delta BIC$ . If judged by the lowest value of  $\chi^2$  the CGR model best describes the HII/GEHR data. The two versions of the standard model,  $\Lambda$ CDM,  $\omega\Lambda$ CDM, perform poorly compared to the  $R_h = ct$  model. We are puzzled by the high values for  $\Omega_m$  in the standard models which are much larger than found earlier using the H-routine with the SNe Ia data [46].

The results in **Table 2** are from data parsed using the 99.99% limits reducing the database by over 40%, though we consider this a conservative parse. The H-routine regressions for all models begins presuming an initial  $H_0$  of 71. The values for  $\Omega_m$  are higher than expected and both the  $R_h = ct$  and CGR models perform poorly describing these data. On the other hand, a version of the current standard model,  $\omega\Lambda$ CDM, performs best considering the  $\Delta BIC$  values but not significantly better than the ST model if one considers the reduces  $\chi^2$  values.

The results in **Table 3** are from data parsed using the Studentised limit discarding values of  $ri/\sigma_i > 1.5$ , which reduces the database a bit further. The  $\omega\Lambda$ CDM, model only slightly outperforms the  $\Lambda$ CDM and ST models with the  $R_h = ct$  model performing poorly. The values for  $\Omega_m$  are all again much higher than expected. Using these parsed data and Eqs. (3), (5), (7), (9), (10) and (13) we can easily discriminate between these more popular models based on the values

Model	$\Delta BIC$	$\chi^2/(N-FP)$	$H_0^a$	$\Omega_m$	Intercept (Mpc)
$\omega\Lambda$ CDM	0	6.04	$65.7 \pm 4.4$	$1 \pm >1000$	-0.07
ST	25.7	5.90	$76.0 \pm 9$	$1 \pm 0.29$	0
$\Lambda$ CDM	27.8	5.98	$76.4 \pm 2.4$	$1 \pm 0.18$	0
CGR	28.3	8.11	$69.2 \pm 1.9$	$1 \pm >1000$	0
$R_h = ct$	43.4	7.22	$73.8 \pm 1.6$	—	0.03
EdS	54.4	6.68	$70.7 \pm 1.7$	1	0.03

<sup>a</sup> $km\ s^{-1}\ Mpc^{-1}$ .

**Table 2.**  
Results from  $D_L$  versus expansion factor with parsed observations including the local group within 99.99% confidence, 89 data pairs.

Model	$\Delta BIC$	$\chi^2/(N-FP)$	$H_0^a$	$\Omega_m$	Intercept (Mpc)
$\omega\Lambda$ CDM	0	2.78	$66.0 \pm >1000$	$1 \pm >1000$	0.02
$\Lambda$ CDM	1.8	2.49	$69.0 \pm 1.6$	$1 \pm 0.15$	0.02
ST	2.9	2.49	$69.5 \pm 1.4$	$1 \pm 0.16$	0.02
EdS	21.3	3.10	$66.1 \pm 1.3$	1	0.02
$R_h = ct$	36.4	4.58	$66.0 \pm 1.$	—	0.02
CGR	41	5.13	$62.3 \pm 2.1$	$1 \pm 0.53$	0

<sup>a</sup> $km\ s^{-1}\ Mpc^{-1}$ .

**Table 3.**  
Results from  $D_L$  versus expansion factor with parsed observations including the local group using a studentised limit of 1.5, 74 data pairs.

calculated for  $\Delta\text{BIC}$ . As expected, the EdS model is too simple and never a good description of the HII/GEHR.

#### 4. Conclusions and discussion

There is a current controversy around the best general description of our Universe. The popular  $\Lambda\text{CDM}$  and  $\omega\Lambda\text{CDM}$  models rely heavily on SNe Ia, Cepheid variable and CMB data for validity as per Riess et al. [9]. Another, the  $Rh = ct$  (the eternal, coasting, non-empty) model functions slightly better than the former two models when tested by proponents with the same SNe Ia data as reported by Wei et al. [55] and with HII/GEHR data [24]. We can reproduce the results of this latter group using their selected data by following the pseudo-H-routine. We acknowledge a serious effort has been made by them to analyse these data using their best techniques, the pseudo-H-routine. Unfortunately their analytical method is flawed, as we have pointed out in our Introduction, leading to questionable results and conclusions by many groups.

We first employ all 156 data pairs organised by Wei et al. [24] with the local group as the origin (1,0) using the H-routine; **Table 1**. Examining **Figures 3** and **4**, the distant data,  $a < 0.85$ , are too scattered with large errors to trust our results so we are forced to use a prior for  $H_0$  as  $71 \text{ km s}^{-1} \text{ Mpc}^{-1}$ . We find the  $Rh = ct$  and CGR models describe the HII/GEHR unparsed data better than the current standard models,  $\Lambda\text{CDM}$  and  $\omega\Lambda\text{CDM}$ . To properly evaluate using the H-routine we are forced to parse the data; this enables the regression procedure to find proper minima. Analyses with the parsed data supports a lower value for  $H_0$  than that of Riess [1], but does not prefer the  $Rh = ct$  model rather the current standard models; **Tables 2** and **3**.

One reason for the discrepancy between parsed and unparsed ensembles is the large dispersion of HII data with large errors for HII distances at  $a < 0.85$  as shown in **Figures 3** and **4**. These large errors are automatically hidden and their influence on regression is drastically increased when the pseudo-H-routine is used, **Figures 1** and **2**. We think the results and conclusions of the Riess [9] and Wei groups [24] are tainted by this type of analysis. If the analyses by these groups be useful and if the pseudo-H-routine be a valid method, our results using the H-routine and the pseudo-H-routine should be similar, but are not [16]. We wonder if the  $Rh = ct$  is really a useful model, since solutions do not present values for cosmological parameters other than  $H_0$ . The  $Rh = ct$  model has other problems as well [28, 36].

The results in **Tables 2** and **3** should not be taken as endorsing the standard model. First, we think the value of the HII/GEHR data, especially events older than  $a \approx 0.85$  is suspect. Second, we have previously shown the complete Einstein field equation, including  $\Lambda$ , when modelled by the FLRW conditions, displays mathematical inconsistencies incompatible with reality [56]. Third, we have recently shown that even  $\Lambda$  tuned to Universe expansion, or tuned to the Hubble-Lemaitre constant, or dependent on decreasing matter density with increasing time, cannot rectify the fundamental problems with that concept [57]. There we have shown by tracing the value of  $\Omega_\Lambda$  back towards recombination demands ridiculous values for either  $\Omega_m$  or  $\Omega_k$  or both. Fourth, the results presented here from analyses of the parsed data with the ST model are as good as the standard model. Finally, an attempt to measure dark energy as a new force failed a sensitive laboratory test [51].

Our picture of the Universe is complicated; when the  $\Lambda\text{CDM}$  model is assayed with CMB data,  $H_0$  is significantly lower ( $66.9 \text{ km s}^{-1} \text{ Mpc}^{-1}$ ) than calculated using SNe Ia data (74.2), both with small claimed errors; [1, 3, 9] but the opposite is expected in a universe suffering gravity. Both the CMB value for  $H_0$  and the



evaluation procedure using that data have been recently, vigorously contested by Riess [7]. In addition to those published arguments, we note that analysis of the CMB data relies on 6 parameters with many required priors, using signal averaged data produced at only a single, distant moment. These are discussion points which are rarely mentioned but which we feel severely weakens the value of the CMB results [11]. On the other hand, we have previously pointed out the SNe Ia data are very noisy, much like the HII/GEHR data shown here [46, 58]. When these data are evaluated with a questionable technique using a 4 or 5 parameter regression in reality, it is not surprising the results from using SNe Ia or HII/GEHR data as standard candles do not always match those of other groups; results from LIGO/Virgo [5, 6].

But why do not astronomers and physicists realise and correct this mistake? The analysis of SNe Ia and HII/GEHR is difficult and time-consuming, thousands of readers prefer to simply trust the results and conclusions of articles written by well-known groups rather than take time and brain-power re-investigating the analyses. But why do astronomers persist in using a system, *mag* versus *z*, which does not yield meaningful results? First, because this is the manner astrophysics was taught and is still followed. Decades ago scientists were forced to plot data in semilog or log-log formats to calculate a value for a rate constant, for instance following a chemical reaction, bygone days when any value was better than none. This practice has been superseded by the use of high-speed computers which can better model relevant data and better calculate rate constants—in our case the Hubble-Lemaître constant. Indeed it has been decades since semilog or log-log plots have been tolerated in biophysics [59]. Astronomy students are not being taught the better techniques of data analysis but the older methods of semilog or log-log plot. Second, data are often organised in tables of redshift and distance magnitude ( $\mu$ ). Both measures are used for historical reasons, magnitude being related to luminosity as perceived by the human eye being approximately the  $\log(\text{luminosity})$ . Some astronomers actually worry more about relatively minor redshift errors than investigate the larger distance errors [37]. Third, results and parameters from this type of analysis (pseudo-H-routine) are interesting and immediately useful in today's astrophysics. The concept of an accelerating Universe expansion due to the release of something like *dark energy* from the spacetime between galactic groups gives the thrill of discovery to astrophysics. This new concept is justification for the billions of \$ spent on large telescopes and satellites, otherwise the money only bought pretty pictures. Fourth, the hope for 'new' physics to young students. This new concept, dark energy, is now fertile ground for theoretical physicists with hundreds of articles published the past 20 years. As a side-note, dozens of articles proposing versions of the MOND model (Modified Newtonian Dynamics) are now defunct, having been dis-proven by the simultaneous observations of light and gravity waves from a binary neutron star collision [60–62]. Fifth, the concept of dark energy has hatched projects employing dozens of astronomers and several large telescopes [63, 64]. Many astronomers are now dedicating time to DES, the Dark Energy Survey, presuming the  $\Lambda$ CDM model correctly describes our Universe [65]. Sixth, many cosmologists and astrophysicist should change their analytical procedures but will not [16]. Finally, the discovery of accelerating Universe expansion has been ennobled with the highest prize for physics [66].

The tension over the correct value of  $H_0$  might be resolved if another set of standard candles, independent of SNe Ia and gamma-ray burst emissions and stretching beyond  $z \approx 2$  could be used for independent model testing with the correct analytic technique, for example, a better quality HII/GEHR data set. Another reason why independent data are needed is because those working with SNe Ia data present the regression for the  $\Lambda$ CDM model as requiring only 2 or 3

parameters; this is really a 4 or 5 parameter regression. (Because the distance data and  $H_0$  must be adjusted between attempted regressions and between models another 2 parameters are introduced making regression a 4 or 5 parameter pursuit. One might term this *data massage*.) In reality, large ensembles of noisy SNe Ia data are only slightly better tools for model discrimination than the ambiguous, 6 parameter fits with CMB data and both SNe Ia and CMB analyses suffer overfitting [11]. Independent data, perhaps from red giants [17], are also important to test the many varieties of dark energy and exotic models now hypothesised to explain the SNe Ia data. These are good reasons why emissions from HII galaxies, GEHR and red giant stars should be seriously considered and encouraged. Extra effort should now be made collecting and analysing many more and better HII/GEHR and red giant signals, the sooner the better, for these data offers a truly independent means of estimating important cosmological parameters. We encourage those collecting and analysing SNe and HII/GEHR data to give more thought to better data analysis and to consider more than just their favourite model.

### Conflict of interest

The authors declare that there exists no conflict of interest.

### Author details


Michael L. Smith<sup>1\*</sup> and Ahmet M. Öztaş<sup>2</sup>

<sup>1</sup> Umeå, Sweden

<sup>2</sup> Department of Physics Engineering, Hacettepe University, Ankara, Turkey

\*Address all correspondence to: mlsmith55@gmail.com

### IntechOpen

© 2020 The Author(s). Licensee IntechOpen. This chapter is distributed under the terms of the Creative Commons Attribution License (<http://creativecommons.org/licenses/by/3.0>), which permits unrestricted use, distribution, and reproduction in any medium, provided the original work is properly cited. 

## References

- [1] Riess AG et al. A 2.4% determination of the local value of the Hubble constant. *The Astrophysical Journal*. 2016;**826**:56. DOI: 10.3847/0004-637X/826/1/56
- [2] Abbott TMC et al. First cosmology results using type Ia supernovae from the dark energy survey: Constraints on cosmological parameters. *The Astrophysical Journal*. 2019;**872**:L30. DOI: 10.3847/2041-8213/ab04fa
- [3] Ade PAR et al. Planck 2015 results—XIII. Cosmological parameters. *Astronomy and Astrophysics*. 2016;**594**:A13. DOI: 10.1051/0004-6361/201525830
- [4] Aghanim N et al. Planck 2018 Results. VI. Cosmological Parameters. 2018. Available from: [arXiv:1807.06209](https://arxiv.org/abs/1807.06209) [Accessed: 20 September 2019]
- [5] LIGO Scientific Collaboration and Virgo Collaboration et al. A gravitational-wave standard siren measurement Hubble constant. *Nature*. 2017;**551**:85–88. DOI: 10.1038/nature24471
- [6] Soares-Santos M et al. First measurement of the Hubble constant from a dark standard siren using the dark energy survey galaxies and the LIGO/Virgo binary-black-hole merger GW170814. *Astrophysical Journal Letters*. 2019;**876**:L7. DOI: 10.3847/2041-8213/ab14f1
- [7] Riess AG et al. Seven Problems with the Claims Related to the Hubble Tension in [arXiv:1810.02595](https://arxiv.org/abs/1810.02595). 2018. Available from: [arXiv:1810.03526](https://arxiv.org/abs/1810.03526)
- [8] Shanks T, Hogarth L, Metcalfe N. *Gaia* cepheid parallaxes and ‘Local Hole’ relieve  $H_0$  tension. *Monthly Notices of the Royal Astronomical Society*. 2018; **484**:L64–L68. DOI: 10.1093/mnras/sly239
- [9] Riess AG et al. Large magellanic cloud cepheid standards provide a 1% foundation for the determination of the Hubble constant and stronger evidence for physics beyond  $\Lambda$ CDM. *The Astrophysical Journal*. 2019;**876**:85. DOI: 10.3847/1538-4357/ab1422
- [10] skydivephil. Cosmology’s Latest Puzzle: The Hubble Tension Featuring Adam Reiss. 2018. Available from: <https://www.youtube.com/watch?v=uoAkFq-Klrk>
- [11] Coolen ACC et al. Replica analysis of overfitting in regression models for time-to-event data. *Journal of Physics A: Mathematical and Theoretical*. 2017;**50**:375001. DOI: 10.1088/1751-8121/aa812f
- [12] Kessler R, Scolnic D. Correcting type Ia supernova distances for selection biases and contamination in photometrically identified samples. *The Astrophysical Journal*. 2017;**836**:56. DOI: 10.3847/1538-4357/836/1/56
- [13] Riess AG et al. New parallaxes of galactic cepheids from spatially scanning the Hubble space telescope: Implications for the Hubble constant. *The Astrophysical Journal*. 2018;**855**:136. DOI: 10.3847/1538-4357/aaadb7
- [14] Huang CD et al. A near-infrared period-luminosity relation for Miras in NGC 4258, an anchor for a new distance ladder. *The Astrophysical Journal*. 2018; **857**:67. DOI: 10.3847/1538-4357/aab6b3
- [15] Vishwakarma RG, Narlikar JV. Is it no longer necessary to test cosmologies with type Ia supernovae? *Universe*. 2018;**4**:73. Available from: <https://www.mdpi.com/2218-1997/4/6/73>
- [16] Smith ML, Oztas AM. Log-transformation Problems. 2017. Available from: <https://www.youtube.com/watch?v=Y1nEQmg2yJA&t=120s>

- [17] Freedman WL et al. The Carnegie-Chicago Hubble program. VIII. An independent determination of the Hubble constant based on the tip of the red giant branch. *The Astrophysical Journal*. 2019;**882**:34. DOI: 10.3847/1538-4357/ab2f73
- [18] Beaton RL et al. The Carnegie-Chicago Hubble Program. VII. The Distance to M101 via the Optical Tip of the Red Giant Branch Method. Available from: arXiv:1908.06120
- [19] Chavez R et al. Determining the  $H_0$  using giant extragalactic HII regions and HII galaxies. *Monthly Notices of the Royal Astronomical Society*. 2012;**425**: L56-L60. DOI: 10.1111/j.1745-3933.2012.01299.x
- [20] Chavez R et al. The  $L\sigma$  relation for massive bursts of star formation. *Monthly Notices of the Royal Astronomical Society*. 2014;**442**: 3565-3597. DOI: 10.1093/mnras/stu987
- [21] Chavez R et al. Constraining the dark energy equation of state with HII galaxies. *Monthly Notices of the Royal Astronomical Society*. 2016;**462**: 2431-2439. DOI: 10.1093/mnras/stw1813
- [22] Terlevich R et al. On the road to precision cosmology with high-redshift HII galaxies. *Monthly Notices of the Royal Astronomical Society*. 2015;**451**: 3001-3010. DOI: 10.1093/mnras/stv1128
- [23] Fernandez Arenas DF et al. An independent determination of the local Hubble constant. *Monthly Notices of the Royal Astronomical Society*. 2017; **474**:1250-1276. DOI: 10.1093/mnras/stx2710
- [24] Wei JJ, Wu XF, Melia F. The HII galaxy Hubble diagram strongly favours  $R_h = ct$  over  $\Lambda$ CDM. *Monthly Notices of the Royal Astronomical Society*. 2016; **463**:1144-1152. DOI: 10.1093/mnras/stw2057
- [25] Leaf K, Melia F. A two-point diagnostic for the HII galaxy Hubble diagram. *Monthly Notices of the Royal Astronomical Society*. 2017;**474**: 4507-4513. DOI: 10.1093/mnras/stx3109
- [26] Yennapureddy MK, Melia F. Reconstruction of the HII galaxy Hubble diagram using gaussian processes. *Journal of Cosmology and Astroparticle Physics*. 2017;**11**:29. DOI: 10.1088/1475-7516/2017/11/029
- [27] John MV, Joseph KB. Generalized Chen-Wu type cosmological model. *Physical Review D*. 2000;**61**:087304. DOI: 10.1103/PhysRevD.61.087304
- [28] John MV.  $R_h = ct$  and the eternal coasting cosmological model. *Monthly Notices of the Royal Astronomical Society*. 2019;**484**:L35-L37. DOI: 10.1093/mnras/sly243
- [29] Melia F, Yennapureddy MK. Model selection using cosmic chronometers with gaussian processes. *Journal of Cosmology and Astroparticle Physics*. 2018;**2**:34. DOI: 10.1088/1475-7516/2018/02/034
- [30] Sandage A et al. The Hubble constant: A summary of the Hubble space telescope program for the luminosity calibration of type Ia supernovae by means of cepheids. *The Astrophysical Journal*. 2006;**653**:843. DOI: 10.1086/508853
- [31] Zheng J, Melia F, Zhang TJ. A Model-independent Measurement of the Spatial Curvature using Cosmic Chronometers and the HII Hubble Diagram. 2019. Available from: arXiv: 1901.05705
- [32] Hubble E. A relation between distance and radial velocity among extra-galactic nebulae. *Proceedings of the National Academy of Sciences of the*



United States of America. 1929;**15**:  
 168-173. DOI: 10.1073/pnas.15.3.168

[33] Feng C et al. Log-transformation and its implications for data analysis. Shanghai Archives of Psychiatry. 2014; **26**:105-109. DOI: 10.3969/j.issn.1002-0829.2014.02.009

[34] Packard GC, Birchard TJ, Boardman TJ. Fitting statistical models in bivariate allometry. Biological Reviews. 2011;**86**: 549-563. DOI: 10.1111/j.1469-185X.2010.00160.x

[35] Packard GC. Relative growth by the elongated jaws of gars: A perspective on polyphasic loglinear allometry. Journal of Experimental Zoology. Part B, Molecular and Developmental Evolution. 2016;**326B**:168-175. DOI: 10.1002/jez.b.22673

[36] Oztas AM, Smith ML. Spacetime curvature and the cosmic horizon: Derivations using the Newtonian world and the Friedmann-Robertson-Walker metric. Monthly Notices of the Royal Astronomical Society. 2015; **449**:1270-1274. DOI: 10.1093/mnras/stv346

[37] Davis TM et al. Can redshift errors bias measurements of the Hubble constant? Monthly Notices of the Royal Astronomical Society. 2019; **490**:2948-2957. DOI: 10.1093/mnras/stz2652

[38] Riazoshams H, Midi H, Gebrenegus G. Robust Nonlinear Regression with Applications Using R. UK: John Wiley; 2019. p. 264

[39] Carroll SM, Press WH, Turner EL. The cosmological constant. Annual Review of Astronomy and Astrophysics. 1992;**30**:499-542. DOI: 10.1146/annurev.aa.30.090192.002435

[40] Carroll SM. The cosmological constant. Living Reviews in Relativity. 2001;**4**:1. DOI: 10.12942/lrr-2001-1

[41] Piattella O. Lecture Notes in Cosmology. UK: Springer Nature; 2018. DOI: 10.1007/978-3-319-95570-4

[42] Melia F, Shevchuk ASH. The  $R_h = ct$  universe. Monthly Notices of the Royal Astronomical Society. 2011;**419**: 2579-2586. DOI: 10.1111/j.1365-2966.2011.19906.x

[43] Riess AG et al. Observational evidence from supernovae for an accelerating universe and a cosmological constant. Astronomy Journal. 1998;**116**: 1009-1038. DOI: 10.1086/300499

[44] Perlmutter S et al. Measurements of  $\Omega$  and  $\Lambda$  from 42 high-redshift supernovae. The Astrophysical Journal. 1999;**517**:565-586. DOI: 10.1086/307221

[45] O’Raifeartaigh C, Mitton S. Interrogating the legend of Einstein’s “Biggest Blunder”. Physics in Perspective. 2018;**20**:318-341. DOI: 10.1007/s00016-018-0228-9

[46] Oztas AM, Smith ML, Paul J. Spacetime curvature is important for cosmology constrained with supernova emissions. International Journal of Theoretical Physics. 2008;**47**:2464-2478. DOI: 10.1007/s10773-008-9680-7

[47] Carmeli M. Relativity: Modern Large Scale Spacetime Structure of the Cosmos. Singapore: World Scientific; 2008. DOI: 10.1142/6820 ISBN 978-981-281-375-6

[48] Hartnett JG. Spiral galaxy rotation curves determined from Carmelian general relativity. International Journal of Theoretical Physics. 2006;**45**:2118-2136. DOI: 10.1007/s10773-006-9178-0

[49] Schumann M. Direct detection of WIMP dark matter: Concepts and status. Journal of Physics G: Nuclear and Particle Physics. 2019;**46**:103003. DOI: 10.1088/1361-6471/ab2ea5

[50] Roberts G Jr. New Results from World’s Most Sensitive Dark Matter



- Detector. Berkeley Lab News Center; 2015. Available from: <https://newscenter.lbl.gov/2015/12/14/new-lux-results/-results/>
- [51] Sabulsky DO et al. Experiment to detect dark energy forces using atom interferometry. *Physical Review Letters*. 2019;**123**:061102. DOI: 10.1103/physrevlett.123.061102
- [52] Schwarz G. Estimating the dimension of a model. *The Annals of Statistics*. 1978;**6**:461-464. Available from: <https://projecteuclid.org/euclid.aos/1176344136>
- [53] Kirshner RK. Hubble's diagram and cosmic expansion. *Proceedings of the National Academy of Sciences of the United States of America*. 2003;**101**:8-13. DOI: 10.1073/pnas.2536799100
- [54] Sandage A, Bedke J. *Atlas of Galaxies*, NASA SP-496, Library of Congress Cataloging-in-Publication Data; 1988
- [55] Wei JJ et al. A comparative analysis of the supernova legacy survey sample with  $\Lambda$ CDM &  $R_h = ct$  universe. *Astronomy Journal*. 2015;**149**:102. DOI: 10.1088/0004-6256/149/3/102/meta
- [56] Oztas AM, Smith ML. Elliptical solutions to the standard cosmology model with realistic matter density. *International Journal of Theoretical Physics*. 2006;**45**:896-907. DOI: 10.1007/s10773-006-9082-7
- [57] Oztas AM, Dil E, Smith ML. The varying cosmological constant: A new approximation to the Friedmann equations and universe model. *Monthly Notices of the Royal Astronomical Society*. 2018;**476**:451-458. DOI: 10.1093/mnras/sty221
- [58] Oztas AM, Smith ML. The cosmological constant constrained with Union2.1 supernovae type data. *International Journal of Theoretical Physics*. 2014;**53**:2636-2661. DOI: 10.1007/s10773-014-2061-5
- [59] Ackers GK. President, American Biophysical Society. Personal communication; 1980
- [60] Boran S et al. GW170817 falsifies dark matter emulators. *Physical Review D*. 2017;**97**:4. DOI: 10.1103/physrevd.97.041501
- [61] Ezquiaga JM, Zumalacarregui M. Dark energy after GW170817: Dead ends and the road ahead. *Physical Review Letters*. 2017;**119**:251304. DOI: 10.1103/physrevlett.119.251304
- [62] Lee C. Colliding Neutron Stars Apply Kiss of Death to Theories of Gravity. 2017. Available from: <https://arstechnica.com/science/2017/10/colliding-neutron-stars-decapitate-zombie-theory-of-gravity/>
- [63] Abbott TMC et al. Dark energy survey year 1 results: A precise  $H_0$  estimate from DES Y1, BAO, and D/H data. *Monthly Notices of the Royal Astronomical Society*. 2018;**480**:3879-3888. DOI: 10.1093/mnras/sty1939
- [64] Abbott TMC et al. Cosmological constraints from multiple probes in the dark energy survey. *Physical Review Letters*. 2019;**122**:17. DOI: 10.1103/physrevlett.122.171301
- [65] Abbott TMC et al. Dark energy survey year 1 results: Cosmological constraints from galaxy clustering weak lensing. *Physical Review D*. 2018;**98**:043526. DOI: 10.1103/physrevd.98.043526
- [66] Riess AG. Nobel lecture: My path to the accelerating universe. *Reviews of Modern Physics*. 2012;**84**:1165-1175. DOI: 10.1103/revmodphys.84.1165